Sensors and Materials, Vol. 36, No. 3 (2024) 831–840
MYU Tokyo

S & M 3565

Visualization of Nutrients and Functional Compounds of Asparagus (*Asparagus officinalis* L.) by Imaging Mass Spectrometry

Mariko Furukawa,[1] Hitomi Shikano,[2] Yukino Watanabe,[3]
Makoto Muto,[2] Daisaku Kaneko,[4] and Shu Taira[2*]

[1]Hama-dori Research Centre, Fukushima Prefectural Agricultural Technology Centre, Narita, Soma 979-2542, Japan
[2]Faculty of Food and Agricultural Sciences, Fukushima University, Kanayagawa, Fukushima 960-1248, Japan
[3]Product Quality and Processing Division, Fukushima Prefectural Agricultural Technology Centre, Hiwada, Koriyama 963-0531, Japan
[4]The Key Laboratory of Synthetic and Biological Colloids, Ministry of Education, School of Chemical and Material Engineering, Jiangnan University, Wuxi, Jiangsu 214122, China

(Received December 12, 2023; accepted February 6, 2024)

Keywords: imaging, food function, asparaptine A, rutin

The nutrient composition of asparagus (*Asparagus officinalis* L.) depends on the harvest period. We visually determined the changes in the relative amounts of asparaptine A and rutin in whole asparagus samples for different harvest periods (May and July) using matrix-assisted laser desorption/ionization (MALDI)–imaging mass spectrometry (IMS). The whole-tissue localization of these functional compounds was determined using longitudinal sections. Asparaptine A was localized throughout the ear tip and stalk regions, and its level was greater in the July harvest period than in the May harvest period. Rutin was localized at the epidermis and exhibited a higher concentration in the early harvest of May, providing protection from UV radiation. For rutin, the relative intensity values of IMS data were in good agreement with the high-performance liquid chromatography (HPLC) data. The combined evaluation of IMS and HPLC has great potential for visually and quantitatively investigating the effects of the harvest period on the nutrient composition and localization and for enhancing commodity values.

1. Introduction

Asparagus (*Asparagus officinalis* L.) is a perennial herb that can be cultivated and harvested continuously for over 10 years, and it is edible as a vegetable. In Japan, it has been cultivated as an agricultural product for the past 150 years. In Fukushima Prefecture, the cultivation of green asparagus began around 1950, and today, it is one of the representative agricultural products of the prefecture.

*Corresponding author: e-mail: staira@agri.fukushima-u.ac.jp
https://doi.org/10.18494/SAM4817

ISSN 0914-4935

Asparagus has two harvest periods: in spring, when young stems that have sprouted using stored nutrients in subterranean stems are harvested, and in summer–autumn, when sprouted young stems are harvested after termination of the spring harvest, during which time the stems and leaves (mother ferns) are actively growing.

Asparagus produces small yellowish-white flowers around May to July. The long, thin, leaf-like growth at the end of the stem is a deformed stem, known as a pseudo-leaf, which is used for photosynthesis. Biologically, the true leaves are the triangular parts attached to the stem, commonly referred to as the *hakama* in Japanese. A previous study investigated the genetic resources and diversity of asparagus.[1]

Asparagus contains polyphenols such as rutin, asparaptine A, and anthocyanins, which exhibit antioxidant properties.[2] Rutin is also one of the nutrient components in asparagus[3] and helps prevent hypertension and arteriosclerosis while also having a diuretic effect.[4] Asparaptine A was isolated in 2015 as a newly discovered component in asparagus.[5] This sulfur-containing metabolite inhibits angiotensin-converting enzyme (ACE), which is associated with hypertension.[5]

It is known that rutin and asparaptine A are present in the ear tip and epidermis. However, no visual information on their longitudinal localization has been reported. Such information would provide valuable nutritional as well as plant physiological data.

Imaging mass spectrometry (IMS) enables the easy identification and provision of such spatial information. Following 2D MS measurements on sample sections at regular intervals, the target signals are reconstructed to obtain an ion image. Thus, IMS enables the simultaneous detection of multiple analytes even in the absence of target-specific markers, such as antibodies,[6–8] in a single experiment. There have been many reports of such studies in fields such as neuroscience,[9–11] pharmacology,[8,12] food chemistry,[13–15] plant science,[16,17] and biology.[18] Here, we aimed to reveal the longitudinal localization of asparaptine A and rutin in asparagus using matrix-assisted laser desorption/ionization time-of-flight (MALDI-TOF)–IMS.

2. Data, Materials, and Methods

2.1 Quantification of rutin by high-performance liquid chromatography (HPLC)

In this study, we selected a new cultivar of asparagus named *Harukitaru*, which is cultivated widely in Fukushima. The asparagus (three-year-old) was harvested at the experimental open field of Fukushima Prefectural Agricultural Technology Centre. The raw samples were harvested in May and July and stored at –80 °C prior to analysis. The frozen spears were cut into six sections (the ear tip region was cut to 4.5 cm and then subsequent sections were cut to 4 cm each). In all experiments, we used four cut sections from the ear tip to the bottom [Fig. 1(a)].

Rutin was extracted from 0.1 g of freeze-dried powder of each section, which was dissolved in 10 mL of 80% methanol and incubated at 80 °C for 10 min. That was repeated three times. Up to 50 mL of the extracted solution was measured and then centrifuged (10000 rpm, 10 min) and filtered (0.45 μm). The rutin content was determined by HPLC using an L-2000 series system (Hitachi High-Tech, Tokyo, Japan) equipped with an Inertsil ODS-3 column (150×4.6 mm I.D., 5

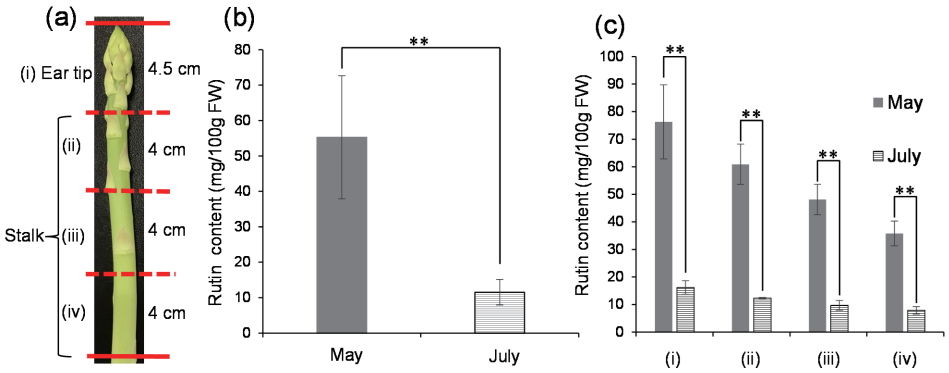

Fig. 1. (Color online) HPLC analysis of rutin in asparagus. (a) Photograph of asparagus (*Asparagus officinalis* L.). Quantitative comparison of the amounts of rutin for May and July: (b) whole asparagus body and (c) at four sites. Obtained values were calculated per unit area. The values are expressed as mean ± standard error. $^{**}p < 0.01$ with Student's *t*-test. $n = 3$.

μm, GL Sciences, Tokyo, Japan). The mobile phase consisted of (A) 2.5% acetic acid (water/acetic acid = 97.5/2.5), (B) acetonitrile, and (C) methanol, (A/B/C = 70/20/10, v/v). Analysis was performed by running each sample for 20 min at a column temperature of 30 °C and a flow rate of 1.0 mL·min^{-1}. Each run was monitored at a wavelength of 350 nm using a UV visible spectrophotometer (Hitachi High-Tech, Tokyo, Japan).

2.2 Preparation of asparagus tissue sections for IMS

The raw asparagus samples were cut in the longitudinal direction for IMS. The cut samples were embedded in a super cryo-embedding medium (SCEM, SECTION-Lab, Hiroshima, Japan) and frozen by freeze-spraying. The specimen block was cut into 30 μm sections using a cryostat (NX70, PHC, Tokyo, Japan) set at –25 °C for the chamber and –23 °C for the object holder. The sections were gently mounted on slides coated with indium tin oxide (ITO; Bruker Daltonics, Billerica, MA, USA). A transfer film (Kawamoto film, SECTION-Lab) was used to prepare the ear tip region sections to maintain the morphology of the asparagus ear. Optical images of the sections were obtained using a scanner (GT-X830, Epson, Tokyo, Japan) prior to MALDI-IMS analysis.

2.3 MALDI-IMS

The matrix α-cyano-4-hydroxycinnamic acid (CHCA; Nacalai Tesque, Japan) solution was prepared as follows. CHCA (60 mg) was dissolved in 6 mL of acetonitrile/water/trifluoroacetic acid (50/49/1, v/v) and sprayed onto the asparagus tissue sections on the ITO-coated glass slides (Bruker Daltonics) using an automated pneumatic sprayer (TM-Sprayer, HTX Tech., Chapel Hill, NC, USA). Ten passes were sprayed with a flow rate of 120 μl·min^{-1}, an air flow of 10 psi, and a nozzle speed of 1100 mm·min^{-1}.

Ionization and imaging of rutin and asparaptine A were confirmed with a MALDI-TOF-MS system (rapifleX, Bruker Daltonics). Tandem MS spectra of sections were obtained using a collision-induced dissociation method. Precursor ion (obtained using 1000 laser shots) and fragment ion (obtained using 4000 laser shots) signals were integrated using flexControl 3.4 software (Bruker Daltonics). Spectra were recorded in positive linear tandem MS mode (voltage of ion source 1: 20 kV; lens voltage: 18 kV). The collision energy was about 1.3 eV, estimated with accelerated voltage using the MALDI TOF/TOF (post source decay: PSD) mode and collision-induced dissociation (CID) via Ar (manufacturer default settings).[19]

For IMS, the laser spot areas were detected by scanning the sections. The laser spot areas (200 shots) were detected with a distance between spot centers of 120 μm in each direction of the asparagus sample. Signals of m/z 100–800 were corrected. The section surface was irradiated with yttrium aluminum garnet (YAG) laser shots in the positive or negative ion detection mode. The laser power was optimized to minimize the in-source decay of the targets. The obtained MS spectra were reconstructed to mass images with a mass bin width of $m/z \pm 0.05$ from the exact mass using flexImaging 5.0 software (Bruker Daltonics). The peak intensity values of the spectra were normalized by dividing by the total ion current to evaluate differences associated with the harvest time from the relative intensity. Imaging area was binarized and calculated using image analysis software (Image J 1.52a).

3. Results and Discussion

3.1 Quantification of asparagus rutin by HPLC

For whole asparagus, samples harvested in May had a 4.8-fold higher rutin content (55.3 ± 17.3 mg/100 gFW) than those harvested in July [11.5 ± 3.6 mg/100 gFW; Fig. 1(b)]. Next, we evaluated the rutin content by region, from the ear tip down (sections i–iv). The data for May revealed that the amount of rutin was highest in the ear tip region (76.3 ± 13.4 mg/100 gFW). The amount of rutin decreased in the order section i > section ii > section iii > section iv [Fig. 1(c)]. Both the whole data and the section data showed significant differences between May and July, indicating that the amount of rutin was less in July than in May. It is known that rutin protects asparagus tissues from UV radiation.[20] In May, the young asparagus stalks are exposed to light radiation because of the absence of leaves. Thus, rutin was localized in the epidermis to protect the tissues from UV radiation. On the other hand, in July, there is less requirement for the active production of rutin because of the shade provided by the standing stalk and the thriving pseudo-leaves. At this time, we did not measure asparaptine A because of the absence of a commercial standard. However, in the IMS experiment, we investigated the localization of rutin and asparaptine A visually. Moreover, we compared the HPLC and IMS data for rutin to identify correlations.

3.2 Detection of targets using MALDI-MS and tandem MS on asparagus sections

In the MALDI-MS analysis of sample sections, we detected the protonated asparaptine A ion at *m*/*z* 307.1 and sodium- and potassium-adducted rutin ions at *m*/*z* 633.1 and 649.2, respectively, in positive ion mode. We confirmed that the detected ions were targeted by tandem MS using the above-detected ions as precursor ions. The precursor ions of the two compounds were cleaved and detected as product ions. In the positive ion mode, the *m*/*z* values of the precursor ions of asparaptine A and rutin were selected to be *m*/*z* 307.1 and 633.1, respectively. The protonated asparaptine A ion was cleaved at the hydroxy group, carboxy group, guanidine group, carbon chains, and 1,2-dithiolane group to provide additional ions. As expected from their chemical structures, the fragment ions were observed at *m*/*z* 290.0, 265.0, 260.0, 249.0, and 175.1 [Fig. 2(a)].

The precursor ion of rutin at *m*/*z* 633.1 was selected as the sodium-adducted ion, whereas the potassium ion was preferentially detected, and it was observed that it seldom cleaved. The sodium ion of rutin was cleaved at the rutinose group and quercetin moiety to provide additional ions. As expected from their chemical structures, the fragment ions were observed at *m*/*z* 331.0 and 324.0 [Fig. 2(b)]. The tandem MS data suggested that the peaks of the precursor ions on the sections detected by MALDI-IMS matched the structures of the target analytes.

3.3 Imaging mass spectrometry

We evaluated the localization of asparaptine A (*m*/*z* 307.1) and rutin as the potassium adduct (*m*/*z* 649.2) using longitudinal and cross sections of asparagus, respectively. From optical images of the asparagus longitudinal and cross sections, we confirmed the presence of the small lateral shoot, epidermis, and asparagus scale (*hakama*), as shown in Fig. 3.

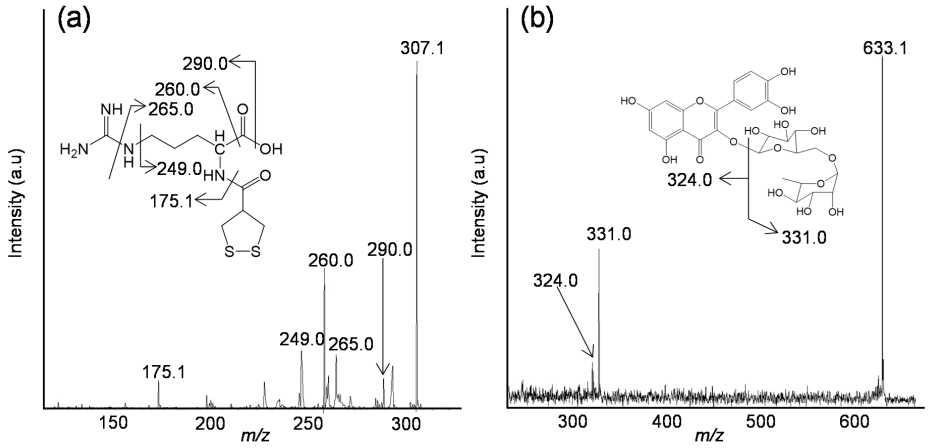

Fig. 2. Tandem mass spectra of selected precursor ions from (a) asparaptine A (*m*/*z* 307.1) as protonated ion and (b) rutin (*m*/*z* 633.1) as sodium-adducted ion.

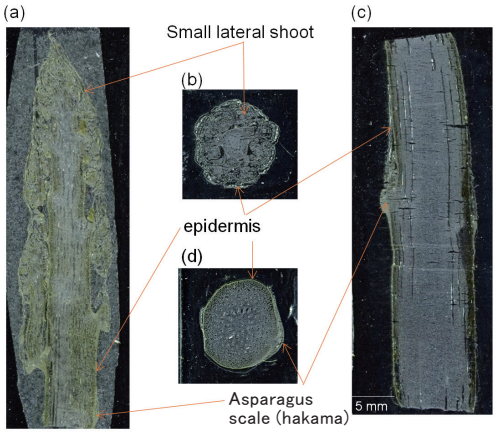

Fig. 3. (Color online) Anatomical photographs of asparagus (*Asparagus officinalis* L.) section. Ear tip region of (a) vertical and (b) ring sections. Stalk region of (c) vertical and (d) ring sections.

In May, asparaptine A was mainly and broadly localized at the ear tip region, and its concentration tended to decrease from the ear tip to the base [Figs. 4(a)–4(c)]. In the stalk regions, asparaptine A was concentrated at the *hakama* (white arrows in Fig. 4). We also confirmed that the localization of functional compounds showed differences between the harvest seasons. In July, the localization of asparaptine A was observed to not change compared with that in May, although in the ear tip region, asparaptine A was mainly concentrated at the small lateral shoot and was localized in the epidermis and scales. In the main body region, it was localized in the inner region of the stalk [Figs. 4(d) and 4(e)].

High-resolution imaging of the cross sections of asparagus indicated that the relative intensities of asparaptine A in the ear tip and stalk sections were 3.4- and 3.7-fold higher in July than in May, respectively [Figs. 4(g) and 4(h)]. This visual information demonstrated that asparaptine A was more concentrated in the small lateral shoot in July than in May. In the stalk region, asparaptine A was observed to localize and increase in concentration in July. Notably, no localization of asparaptine A in the vascular bundles was observed; however, localization around the vascular bundles in the stalk region and asparagus scales was observed [Fig. 4(h)]. Thus, asparaptine A may be produced in different plant cells and used to promote growth. In addition, to confirm whether there is an effect of ion suppression between samples or not, the data of ring sections from May and July asparagus was helpful. As the results were the same as those of the longitudinal sections, it was determined that the effect of ionization suppression was minimal.

Rutin was localized in the small lateral shoot in the ear tip region and in the epidermis of sections from the top to the bottom in May [Figs. 5(a)–5(c)]. In a comparison of rutin by harvest season, it was observed that in both longitudinal and cross sections, the MS signal intensity for rutin decreased from the ear tip and was weakly imaged in the epidermis in July [Figs. 5(d)–5(f)]. The rutin intensity in May was 8.2- and 3.9-fold greater in the ear tip and stalk sections, respectively, than those in July. This is attributed to the cultivation method of asparagus. Asparagus is a perennial herb that consists of the underground culm and rhizome. The rhizome

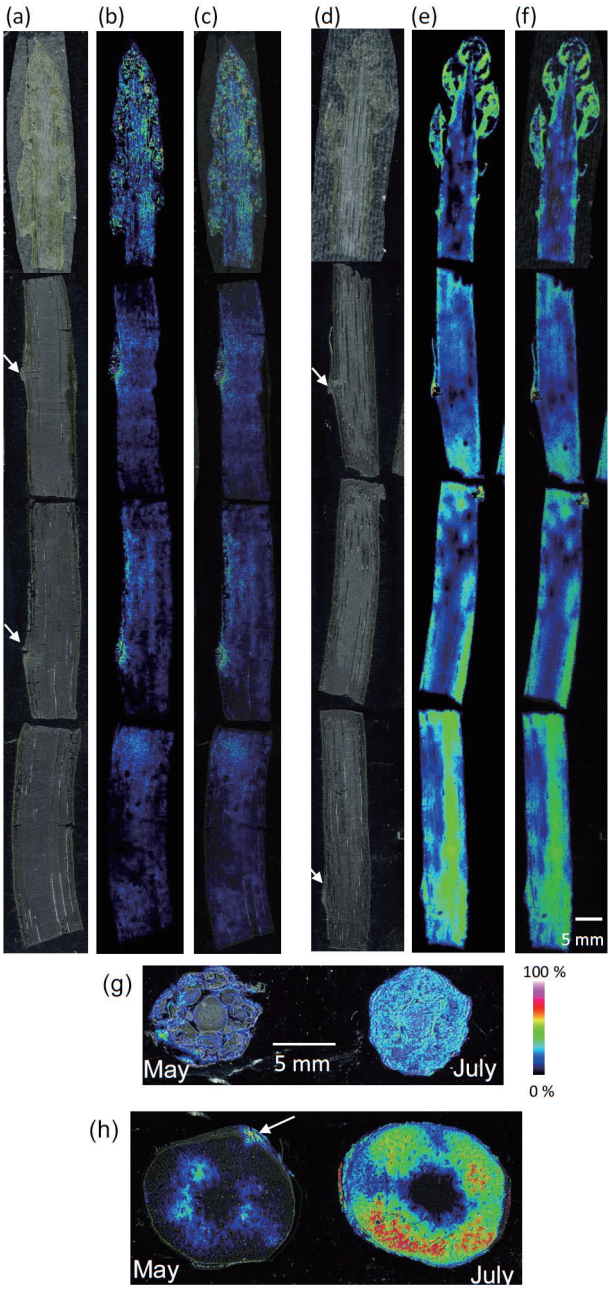

Fig. 4. (Color online) Mass spectral image of asparaptine A in asparagus. Optical image of the asparagus vertical section for (a) May and (d) July; IMS of asparaptine A (*m*/*z* 307.1) for (b) May and (e) July; merged image obtained from optical image and ion image for asparaptine A for (c) May and (f) July. Merged image obtained from optical ring image and ion image for asparaptine A in (g) ear tip region and (h) stalk.

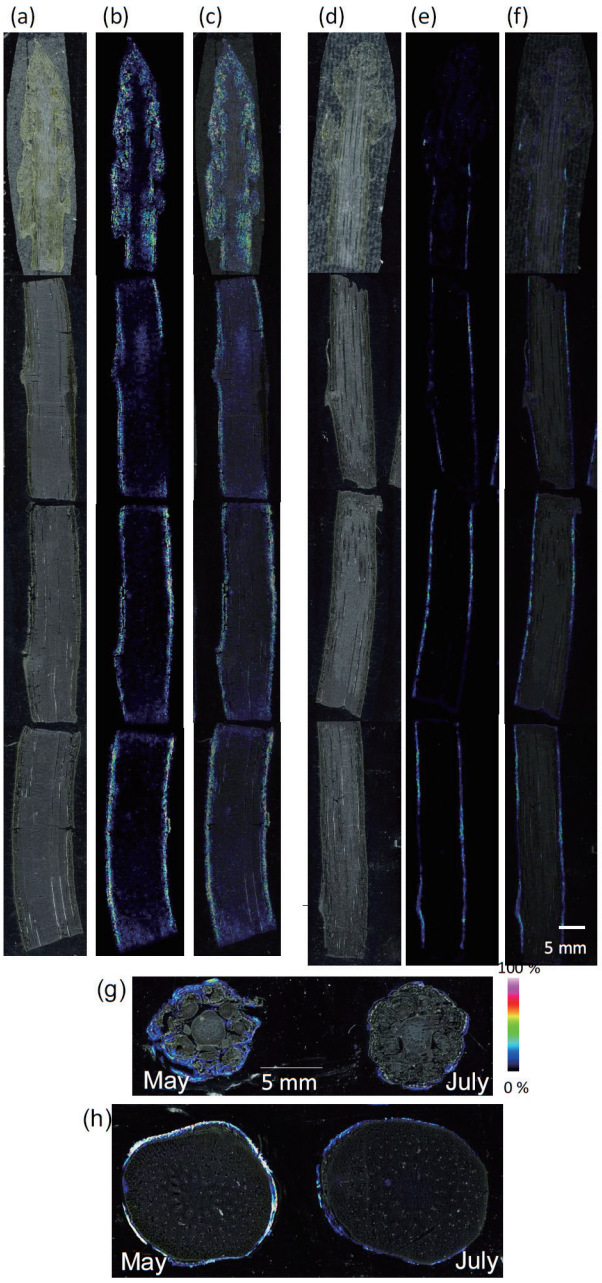

Fig. 5. (Color online) Mass spectral image of rutin in asparagus. Optical image of the asparagus vertical section for (a) May and (d) July; IMS of rutin (*m*/*z* 633.1) for (b) May and (e) July, merged image obtained from optical image and ion image for rutin for May (c) and (f) July. Merged image obtained from optical ring image and ion image for rutin at (g) ear tip region and (h) stalk.

elongates in the horizontal direction in the ground and the culm grows upward. As mentioned previously, rutin protects plant tissues from UV radiation. During growth in May, abundant rutin is produced in the plant in response to the immature leaf growth and lack of shade from the sun, thereby protecting itself from UV damage.

4. Conclusions

In summary, we demonstrated that we were able to assess the seasonal variation of the components of asparagus by IMS. MALDI-IMS was able to detect and image asparaptine A and rutin on sample sections. We were also able to demonstrate that the distributions of these metabolites changed between the May and July harvest times. Notably, the high-resolution IMS data suggested that asparaptine A is not made and transported in the rhizome but is produced in plant cells of the whole body [Figs. 4(g) and 4(h)]. Quantification by MALDI-IMS is challenging because the signal intensity depends on many factors; thus, we determined the rutin content by HPLC, which was in good agreement with the IMS data. IMS and HPLC are powerful tools for the direct visualization and quantification of biological samples to reveal plant physiology as well as vital functions.

Acknowledgments

This work was supported by "Reconstruction and Revitalization of the Agriculture, Forestry and Fisheries in Fukushima Prefecture" project.

References

1 T. Nothnagel, H. Budahn, I. Krämer, E. Schliephake, E. Lantos, S. Plath, and R. Krämer: Genet. Resour. Crop Evol. **64** (2017) 1873. https://doi.org/10.1007/s10722-016-0476-y
2 R. Fan, F. Yuan, N. Wang, Y. Gao, and Y. Huang: J. Food Sci. Technol. **52** (2015) 2690. https://doi.org/10.1007/s13197-014-1360-4
3 S. Motoki, T. Tang, T. Taguchi, A. Kato, H. Ikeura, and T. Maeda: HortScience **54** (2019) 1921. https://doi.org/10.21273/HORTSCI14131-19
4 D. Vora, J. D. Vora, S. R. Pednekar, and R. R. Khadke: J. Biotechnol. Biochem. **3** (2017) 83
5 R. Nakabayashi, Z. Yang, T. Nishizawa, T. Mori, and K. Saito: J. Nat. Prod. **78** (2015) 1179. https://doi.org/10.1021/acs.jnatprod.5b00092
6 S. Taira, Y. Sugiura, S. Moritake, S. Shimma, Y. Ichiyanagi, and M. Setou: Anal. Chem. **80** (2008) 4761. https://doi.org/10.1021/ac800081z
7 M. Stoeckli, P. Chaurand, D. E. Hallahan, and R. M. Caprioli: Nat. Med. **7** (2001) 493. https://doi.org/10.1038/86573
8 S. Taira, R. Ikeda, N. Yokota, I. Osaka, M. Sakamoto, M. Kato, and Y. Sahashi: Am. J. Chin. Med. **38** (2010) 485. https://doi.org/S0192415X10008007
9 Y. Tatsuta, K. Kasai, C. Maruyama, Y. Hamano, K. Matsuo, H. Katano, and S. Taira: Sci. Rep. **7** (2017) 12990. https://doi.org/10.1038/s41598-017-13257-8
10 M. Shariatgorji, A. Nilsson, Richard J. A. Goodwin, P. Källback, N. Schintu, X. Zhang, Alan R. Crossman, E. Bezard, P. Svenningsson, and Per E. Andren: Neuron **84** (2014) 697. https://doi.org/http:/dx.doi.org/10.1016/j.neuron.2014.10.011
11 Y. Sugiura, R. Taguchi, and M. Setou: PLoS One **6** (2011) e17952. https://doi.org/10.1371/journal.pone.0017952
12 R. Wang, T. Yamada, S. Arai, K. Fukuda, H. Taniguchi, A. Tanimoto, A. Nishiyama, S. Takeuchi, K. Yamashita, K. Ohtsubo, J. Matsui, N. Onoda, E. Hirata, S. Taira, and S. Yano: Molecular Cancer Therapeutics **18** (2019) 947. https://doi.org/10.1158/1535-7163.mct-18-0695

13 M. Shiota, Y. Shimomura, M. Kotera, and S. Taira: Food Chem. **245** (2018) 1218. https://doi.org/https:/doi.org/10.1016/j.foodchem.2017.11.009
14 M. Ha, J. H. Kwak, Y. Kim, and O. P. Zee: Food Chem. **133** (2012) 1155. https://doi.org/http:/dx.doi.org/10.1016/j.foodchem.2011.11.114
15 T. Hase, S. Shishido, S. Yamamoto, R. Yamashita, H. Nukima, S. Taira, T. Toyoda, K. Abe, T. Hamaguchi, K. Ono, M. Noguchi-Shinohara, M. Yamada, and S. Kobayashi: Sci. Rep. **9** (2019) 8711. https://doi.org/10.1038/s41598-019-45168-1
16 K. Shiono, R. Hashizaki, T. Nakanishi, T. Sakai, T. Yamamoto, K. Ogata, K.-i. Harada, H. Ohtani, H. Katano, and S. Taira: J. Agric. Food Chem. **65** (2017) 7624. https://doi.org/10.1021/acs.jafc.7b02255
17 L. Huang, X. Tang, W. Zhang, R. Jiang, D. Chen, J. Zhang, and H. Zhong: Sci. Rep. **6** (2016) 24164. https://doi.org/10.1038/srep24164
18 M. L. Steinhauser, A. P. Bailey, S. E. Senyo, C. Guillermier, T. S. Perlstein, A. P. Gould, R. T. Lee, and C. P. Lechene: Nature **481** (2012) 516. https://doi.org/http:/www.nature.com/nature/journal/v481/n7382/abs/nature10734.html (supplementary-information)
19 K. F. Medzihradszky, J. M. Campbell, M. A. Baldwin, A. M. Falick, P. Juhasz, M. L. Vestal, and A. L. Burlingame: Anal. Chem. **72** (2000) 552. https://doi.org/10.1021/ac990809y
20 D. Z. K. Wambrauw, T. Kashiwatani, M. Matsuhashi, S. Yasuhara, S. Oku, H. Shimura, K. Honda, T. Maeda, and T. Yamaguchi: Environ. Control Biol.. **59** (2021) 191. https://doi.org/10.2525/ecb.59.191